Thickness and structure of thin films determined by background analysis in hard X-ray photoelectron spectroscopy

Yi-Tao Cui,[1,a),b)] Sven Tougaard,[2] Hiroshi Oji,[1,3] Jin-Young Son,[1,3] Yasuhiro Sakamoto,[4,5] Takuya Matsumoto,[1,3] Anli Yang,[6] Osami Sakata,[6] Huaping Song,[7] and Ichiro Hirosawa[1]
[1]*Japan Synchrotron Radiation Institute, 1-1-1 Kouto, Sayo-cho, Sayo-gun, Hyogo 679-5198, Japan*
[2]*Department of Physics, Chemistry and Pharmacy, University of Southern Denmark, DK-5230 Odense M, Denmark*
[3]*SPring-8 Service Co., Ltd., 2-23-1 Kouto, Kamigori-cho, Ako-gun, Hyogo 678-1205, Japan*
[4]*Nanoscience and Nanotechnology Research Center, Research Organization for the 21st Century, Osaka Prefecture University, 1-2 Gakuen-cho, Naka-ku, Sakai 599-8570, Japan*
[5]*Precursory Research for Embryonic Science and Technology (PRESTO), Japan Science and Technology Agency (JST), 4-1-8 Honcho, Kawaguchi, Saitama 332-0012, Japan*
[6]*Synchrotron X-ray Station at SPring-8, National Institute for Materials Science, 1-1-1 Kouto, Sayo-cho, Sayo-gun, Hyogo 679-5148, Japan*
[7]*Research Institute, Kochi University of Technology, Kami, Kochi 782-8502, Japan*

(Received 19 January 2017; accepted 25 May 2017; published online 13 June 2017)

We report on the analysis of inelastic backgrounds associated with photoelectron peaks from thin films of Ru on Si using hard X-ray photoelectron spectroscopy (HAXPES) with an X-ray energy of 7939 eV. To extract information on the thickness and morphology of the Ru films, the Tougaard-background-analysis method was used. Consistent results from the analysis of the Si 1*s* peaks as well as the Ru 2*p*, 2*s* peaks to the thicknesses determined with X-ray reflectivity were found. Good agreement was also found for surface topography (the Ru forms islands on the Si surface for film thicknesses <12 nm and covers the complete surface for larger thicknesses) determined by our fitting results and scanning electron microscopy. It is demonstrated that with this method it is possible to obtain information on films up to 150 nm thickness, which corresponds to ~20 times the inelastic mean free paths (IMFPs). This is larger than the previously reported ~10 times the IMFP for X-ray photoelectron spectroscopy with conventional X-ray sources owing to the fact that the spectrum can be followed over a larger range of energy-loss. The method can also be used to determine the IMFP if the film thickness is known by another technique and it was applied to determine the IMFP for Ru at 4900 eV (4.3 nm) and 6050 eV (5.3 nm). In addition, some possible applications of the methods are described. *Published by AIP Publishing*. [http://dx.doi.org/10.1063/1.4985176]

INTRODUCTION

About thirty years ago, Tougaard[1] pointed out that the peak shape in X-ray photoelectron spectroscopy (XPS) spectra is strongly dependent on the depth of the corresponding element in the solid. By analyzing the background of inelastically scattered electrons, one can obtain information on the depth distribution of atoms up to ~10 times as large as the inelastic electron mean free path (IMFP, λ),[2,3] which is much larger than that can be obtained by peak-intensity analysis (<3λ and in favorable cases <5 λ). In the present paper, we demonstrate that for hard X-ray photoelectron spectroscopy (HAXPES) of Ru, information for depths up to 20 IMFP can be obtained because the inelastically scattered electrons can be followed over a 500 eV energy range. The method has been extensively applied to the quantitative non-destructive analysis of depth and structural profiling of nanostructures by soft X-ray XPS spectra (e.g., with Al or Mg K_α X-ray sources).[3] As it is well known, the XPS signal excited by soft X-rays is surface sensitive due to the relatively low electron kinetic energy, which limits the applications of soft X-ray XPS for *ex-situ* prepared thin films or nano-particles without sample cleaning. Recent advances in X-ray undulator technology at third-generation synchrotron light sources enable the delivery of an unprecedented high photon flux,[4,5] which can well compensate for the reduction of photoionization cross section and analyzer transmission, and make high-energy, high-resolution HAXPES accessible.[6–8] Since then, HAXPES has been quickly developed and has been applied to research in a wide range of fields.[9] The relatively large IMFP of photoelectrons with higher kinetic energy facilitates studies of the electronic structure of bulk materials, nano-scale buried layers, and their interfaces since the relative contribution of signals from the surface region is reduced in HAXPES compared with that in soft X-ray XPS.[10] The absorbed carbon contaminants on a Si wafer are typically around 0.6 nm (and even with a smeared thumbprint around 2 nm of contaminants is formed on Si wafer surfaces)[11] but the high photon energy excites high kinetic energy electrons with an IMFP much larger than 1 nm. This situation implies that HAXPES can be used even without careful surface

[a)]Present address: Synchrotron Radiation Laboratory, Laser and Synchrotron Research Center (LASOR), The Institute for Solid State Physics, The University of Tokyo, 1-490-2 Kouto, Shingu-cho Tatsuno, Hyogo 679-5165, Japan
[b)]yitaocui@issp.u-tokyo.ac.jp

cleaning. As seen in Fig. 1(a), IMFP (calculated with the TPP-2M formula[12–14]) at high kinetic energies such as 8 keV is in the 5–16 nm range. This fact opens up structures at depths up to ~100 nm for non-destructive analysis by HAXPES since the relative contributions from layers beneath the surface layer are much enhanced in comparison with spectra from conventional laboratory XPS with X-ray tubes as shown in Fig. 1(b).

In this work, several different methods for evaluating the thicknesses of thin films were applied to model samples in order to confirm the possibility of the background-analysis method, and the results were examined in detail. Therefore, information such as the thicknesses and structures of thin films, electron IMFPs in the film, and other intrinsic properties could be determined. The analysis of the inelastic background combined with HAXPES was recently successfully applied to HAXPES of a deeply buried Ti layer in the 14 to 25 nm depth range.[15]

EXPERIMENT

The Ru thin-film samples were commercially obtained from NTT Advanced Technology Corporation, Japan. These samples were made by the sputter deposition method on a clean 4-in. Si (100) wafer surface with target thicknesses of 3 nm, 9 nm, 15 nm, 100 nm, and 150 nm and are designated as Ru/Si A, Ru/Si B, Ru/Si C, Ru/Si D, and Ru/Si E, respectively. All samples together with the Si (100) wafer were cut into 5 mm × 5 mm pieces and then fixed to a Cu holder by carbon conducting tapes for HAXPES measurements.

HAXPES measurements were carried out at the undulator beamline BL46XU of SPring-8.[16,17] The excitation X-ray beam used for HAXPES was monochromatized with a Si (111) double-crystal and Si (444) channel-cut monochromators, which provide an X-ray energy resolution of 40 meV at ~7939 eV (Ref. 18) with a focal spot size of 0.02 mm (vertical) × 0.2 mm (horizontal) and a photon flux of $\sim 2 \times 10^{11}$ photons/s. A VG Scienta R4000 hemispherical electron analyzer for high electron kinetic energies (up to 10 keV) with an acceptance angle of ±8° was used. In order to remove non-dipole effects, the analyzer was fixed at the parallel direction of the X-ray polarization. The take-off-angle (TOA) of photoelectrons with respect to the sample surface was set to 80°. A curved slit with a width of 0.5 mm was used and the analyzer pass energy was fixed at 200 eV, which results in a total energy resolution of 230 meV. The experiments were carried out at room temperature with the vacuum better than $\sim 5 \times 10^{-6}$ Pa in the analysis chamber.

To evaluate the thickness and surface condition of the samples, scanning electron microscopy (SEM), atomic force microscopy (AFM), and X-ray reflectivity (XRR) measurements were performed. For the SEM experiment, a JEOL system was used with an electron-acceleration voltage of 15 kV. The surface morphology was characterized by atomic force microscopy (AFM) using JEOL JSPM-5200. For the XRR experiments, all samples were measured with a laboratory XRR system with Cu $K\alpha$ X-rays after fabrication and then confirmed with synchrotron-based systems in beamlines BL46XU and BL15XU with X-ray energies of 10 keV and 12.4 keV, respectively.

The background fits were performed with the QUASES-Tougaard software.[19] XRR results were fitted with GIXRR software for reflectivity analysis (Rigaku Corp.).

RESULTS AND DISCUSSION

Survey spectra of Ru thin-film samples excited by 7939 eV X-rays are shown in Fig. 2. As seen in the figure, the peak intensities of the Ru core-level peaks (2*s*, 2*p*, 3*s*, 3*p*, 3*d*, etc.) increase and the Si peak intensities (1*s*, 2*s*, 2*p*, etc.) decrease as the Ru thickness increases, indicating the reduction of the Si signal by energy-loss processes in the Ru film. The Si 1*s* and Ru 2*s* 2*p* core-level spectra (normalized to the Si 1*s* and Ru $2p_{3/2}$ peak intensities, respectively) are shown in Figs. 3(a) and 3(b), respectively. The inelastic backgrounds from both Si and Ru core-level spectra are enhanced with increasing Ru thickness. This background enhancement and changes in the shape of the spectra come from inelastic energy loss of photoelectrons during travel from where they were excited in deeper layers to the surface of the sample. As pointed out by Tougaard,[1–3] the relationship of background and peak intensity (in other words, the spectral shape) can be used to determine the film structure by analysis with different models. The method neglects elastic-

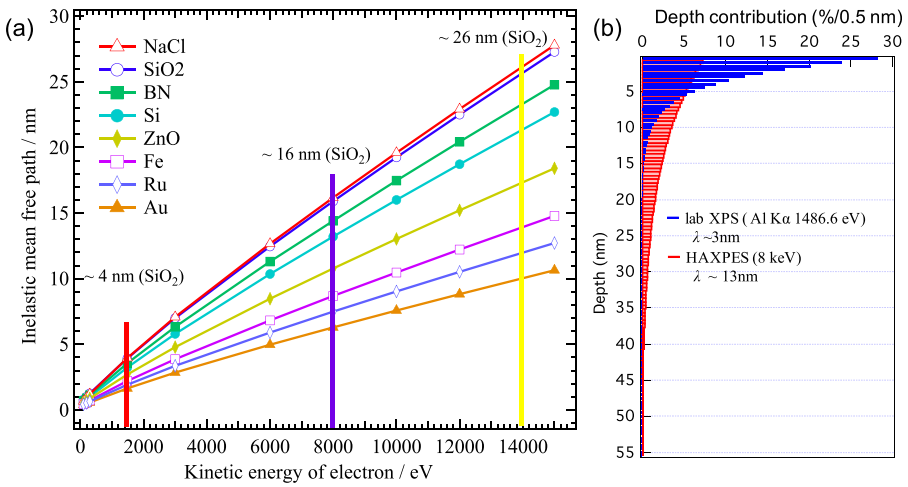

FIG. 1. (a) Inelastic mean free paths of photoelectrons for typical samples as a function of electron kinetic energy. (b) The comparison of depth contributions between laboratory XPS and HAXPES for SiO_2.

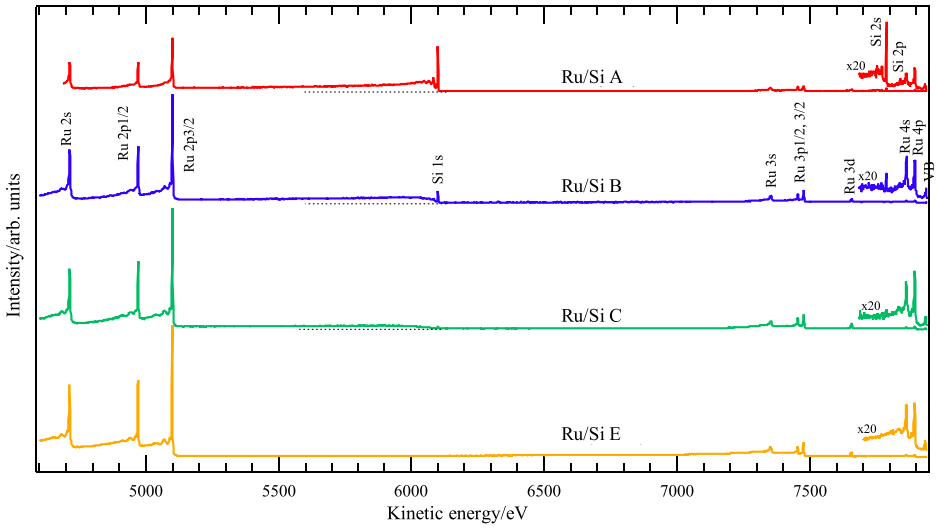

FIG. 2. Survey spectra with different Ru thicknesses on Si (100) substrates. The dotted lines were drawn parallel to zero line to clearly show the background differences around Si 1*s* peaks.

electron scattering which is likely to be a good approximation, in particular, at the high electron energies considered here.[3]

The background analysis can be performed using an algorithm that removes the background of inelastically scattered electrons (this is done with the Analyze part of the QUASES-Tougaard software[19]), referred to as "method A," hereafter. Alternatively, the analysis can be done by calculating the inelastic background (with the Generate part of the software), referred to as "method B" hereafter. The shape and intensity of the background depend critically on the depth distribution of the selected atoms. By comparison to the experimental spectrum, this relationship can be determined from simulations with certain models. Thus for method A, one starts with the measured spectrum $J(E)$ and calculates the background using different model depth distributions.[3] This results in the background corrected spectrum $F'(E)$ which is the atomic spectrum at the point of excitation

$$F'(E) = \frac{1}{P_1}\left\{J(E) - \int dE' J(E) \int ds e^{i2\pi s(E'-E)}\left(1 - \frac{P_1}{P(s)}\right)\right\}, \quad (1)$$

$$P(s) = \int dz c(z) e^{-\frac{z}{\lambda \cos\theta}\sum(s)}; \quad P_1 = \int dz c(z) e^{-\frac{z}{\lambda\cos\theta}};$$
$$\sum(s) = \frac{1}{\lambda} - \int_0^\infty dT \cdot K(T) e^{-isT}, \quad (2)$$

where $J(E)$ is the measured spectrum, $F'(E)$ is the excitation spectrum from a single atom at the point of excitation in the solid (i.e., the spectrum without inelastic background caused by photoelectrons passing through layers), $c(z)$ is the concentration of atoms as a function of depth z, $K(T)$ is the cross section for an electron of energy E_0 to lose energy T, θ is the emission angle with respect to the sample normal, and λ is the IMFP of photoelectrons at energy E_0. The IMFP (λ) can be generated by the TPP-2M formula.[12–14] The cross section for energy loss $K(T)$ depends to some extent on the material[20] and can usually be estimated from different universality classes of cross sections. For most transition metals, their alloys and oxides, Tougaard's universal cross section can be applied with reasonable accuracy.[20] Some materials such as Al and Si have very sharp plasmon excitations and for such materials it is more accurate to use the three parameter-universal cross section.[20] The universal cross section and the three parameter-universal cross section for

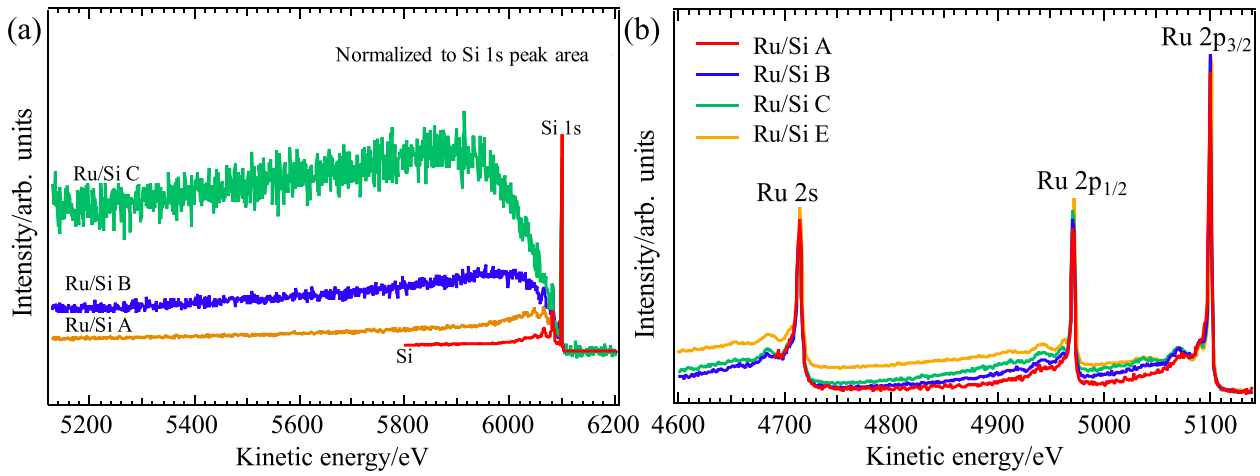

FIG. 3. The normalized (a) Si 1*s* and (b) Ru 2*s* and 2*p* core-level spectra for different samples on Si (100) substrates.

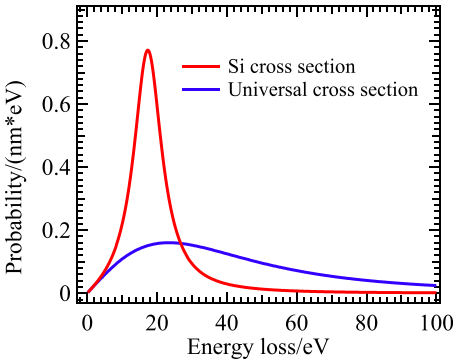

FIG. 4. The energy-loss three parameter-universal cross section of Si and the universal cross section for transition metals such as Ru (from Ref. 19).

silicon used here to calculate energy loss in Ru and Si layers, respectively, are shown in Fig. 4.

Based on method A, the fitting results of Ru 2*s*, 2*p* core-level spectra are shown in Fig. 5. Here, the only unknown parameter is the Ru thickness. This is varied until the background of inelastically scattered electrons is accounted for over a wide energy range below the peaks. The fact that this is possible and that the fitting of the background intensity is very good over an energy range of ∼500 eV implies that the Ru is indeed present as a layer on top of the Si substrates. The Ru overlayer thickness is determined in this manner. Up to this point, we have not used any information on the absolute peak intensities but only the relative intensities between the elastic (peak) intensity and the inelastically scattered electrons in the background. Therefore, we have determined the depth distribution but not the concentration of Ru. Thus, if Ru forms islands on the surface, different coverages will lead to different intensities. To determine the coverage, the absolute intensity scale must be fixed. This is done with the use of a reference spectrum from a thick Ru sample. This

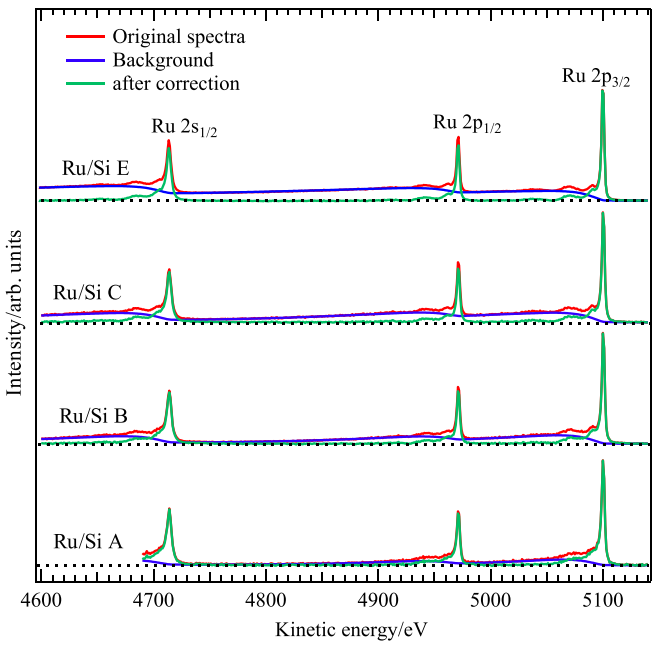

FIG. 5. The fitting results of Ru 2*s* and 2*p* core-levels by method A. The dotted lines mark the zero intensity of each spectrum.

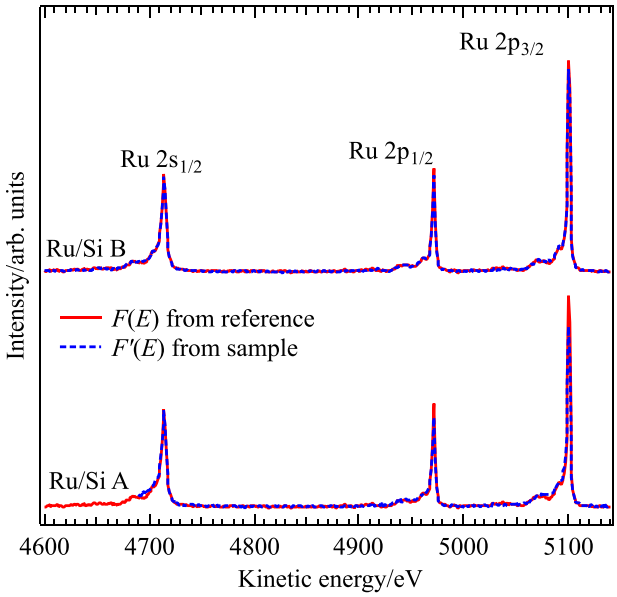

FIG. 6. Comparison of calculated $F'(E)$ with a reference $F(E)$ on a relative scale for Ru/Si A and Ru/Si B.

spectrum can be analyzed accurately since we know the depth distribution for this sample (constant Ru concentration for all depths), and in this way, we determine the absolute atomic spectrum, $F(E)$, for Ru. The analyzed spectra $F'(E)$ must then match this reference $F(E)$ both with respect to shape and intensity. The comparison of the two spectra is done directly within the QUASES-software and final adjustments of both the Ru layer thickness and the coverage are made until $F'(E) \simeq F(E)$ over a wide energy range, i.e., they match on an absolute scale both with respect to intensity and shape as shown in Fig. 6. The determined Ru thicknesses, coverages, and average Ru thicknesses are listed in Table I. The agreement between $F(E)$ and $F'(E)$ in Fig. 6 is excellent, and the determined coverages are also consistent with the surface topography determined by SEM as shown in Figs. 7(a), 7(b), 7(c), and AFM images (not shown). The results show that the Ru film on the Ru/Si A sample forms islands that cover 64% of the Si surface. The coverage increases to 97.3% for Ru/Si B, while for samples Ru/Si D, E, and F, the Si substrate is completely covered by the Ru films with a flat surface.

Figure 8 shows a similar analysis of the Si 1*s* spectra with method A using the IMFP of Ru and the universal

TABLE I. Ru thicknesses, surface Ru coverage, and average Ru thicknesses from the fits of Ru 2*s*, 2*p* core-level peaks with method A for each sample. The IMFPs used for the fits were 4.77 nm at the kinetic energy of 4900 eV around the Ru $2p_{3/2}$ peak generated with Eq. (7) and the parameters in Tables 2 and 5 of Ref. 12.

Sample	Ru thickness (nm)	Coverage (%)	Average thickness (nm)
Ru/Si A	6.5	64	4.2
Ru/Si B	12.0	97.3	11.7
Ru/Si C	17.0	100	17.0
Ru/Si D	>100	100	>100
Ru/Si E	>100	100	>100

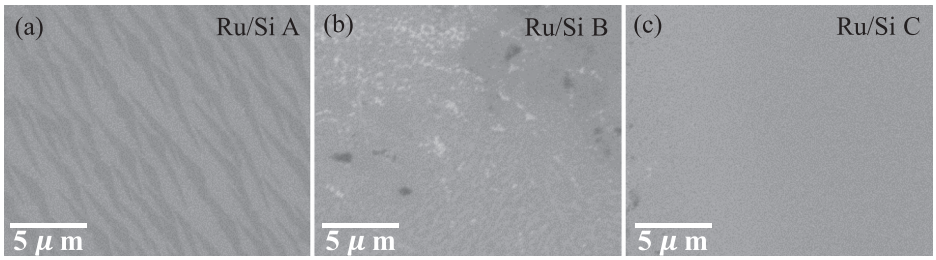

FIG. 7. SEM images of samples (a) Ru/Si A, (b) Ru/Si B, and (c) Ru/Si C. For all SEM images, a 15 kV electron-acceleration voltage was used.

energy-loss cross section (Fig. 4). It is seen in Fig. 8(a) that the background accounts quite well for the intensity far away from the peak (energy loss > 100 eV) but does not fit so well in the energy region close to the peak (energy loss < 100 eV) as shown in Fig. 8(b). This result is due to large differences in the cross section for electron energy loss $K(T)$ (see Fig. 4) as well as the IMFP for the two materials (Si and Ru). The results in Fig. 8 can be understood as follows: for large energy loss (>100 eV), the electrons have undergone several inelastic scattering events and the structure in the cross section is smeared out, while for smaller energy loss, the electrons have typically only undergone one or two energy-loss events and details of the cross section play a more prominent role. The large deviations at energies <50 eV from the Si 1*s* peak for the thinner samples (Ru/Si A and B) are due to the larger relative contribution from the Si substrate to the energy-loss distribution.

In the case of the Si 1*s* spectrum, the photoelectrons pass through the Si first and then the Ru overlayer, where both the IMFPs and the cross sections are significantly different [see Figs. 1(a) and 4, respectively]. Actually, inversely, one can in principle generate the spectrum ($J(E)$) from the $F(E)$ of the pure Si spectrum by using the appropriate cross sections and IMFPs of different layers[3]

$$J(E) = \int dE_0 \cdot F(E_0) \int_0^{\infty} c(z) \cdot G\left(E_0, \frac{z}{\lambda \cos\theta}; E\right) dz, \quad (3)$$

$$G(E_0, R; E) = \frac{1}{2\pi} \int_{-\infty}^{\infty} e^{is(E_0 - E) - R\sum(s)} ds, \quad (4)$$

where $J(E)$ is the generated spectrum after passing certain layer(s) and $F(E)$ is the original spectrum without inelastic background. In the Quases-Generate software,[19] this is done by calculating the effect of transporting the spectrum from pure Si through the overlayer Ru film structure. Thus, only the IMFP and the cross section for Ru is an input in this calculation. Finally, this Si 1*s* spectrum including the background of inelastically scattered electrons is calculated after it has been transported through the Ru overlayer and this spectrum is compared directly to the measured Si 1*s* spectrum. Thus, with method B, one can start with the spectrum of pure Si and calculate the changes as the electrons pass through the Ru overlayer. This procedure has the advantage that the only material parameters involved in the calculation are the cross section and IMFP for Ru. The Ru overlayer thickness was adjusted until the best agreement with the measured Si 1*s* spectra (compared on an absolute scale) was found. The resulting spectra plotted in Fig. 9 show that the background is now in very good agreement with experiment also for energies <50 eV from the Si 1*s* peak. The determined thicknesses are listed in Table II (named as Method B). The results from analysis of the Ru spectra (Table I) are also shown in Table II.

For comparison, the thicknesses of the Ru films were evaluated with conventional methods such as by XRR as

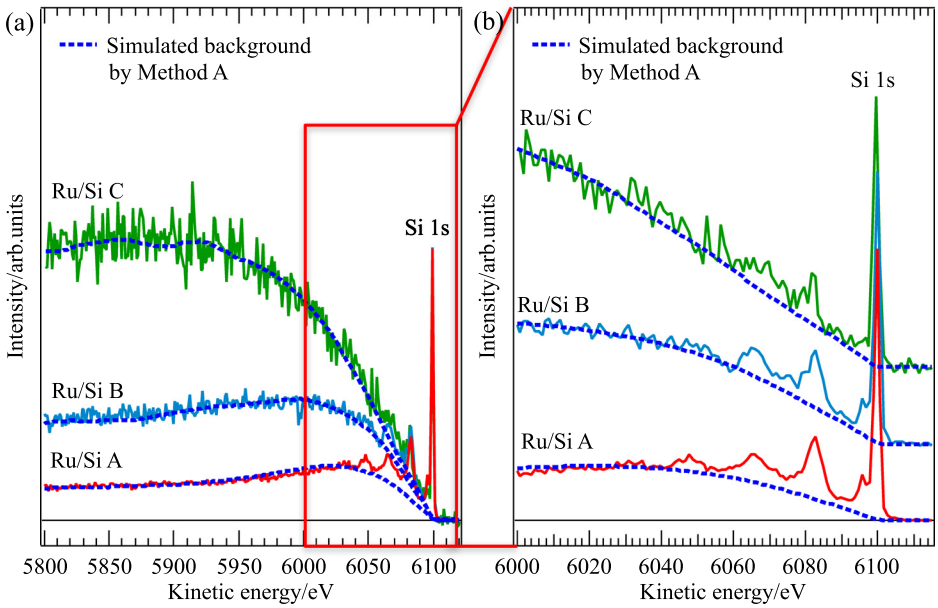

FIG. 8. The background fitted with method A using the Ru universal cross section and the IMFP of 5.68 nm (around Si 1*s* for Ru) (dashed lines) against the measured spectra (solid lines) around the Si 1*s* peak. (a) The best fit over a wide energy region. (b) Close view in the near Si 1*s* peak region. The mismatch near the Si 1*s* peak is due to the differences in energy-loss cross section and IMFPs between Si and Ru.

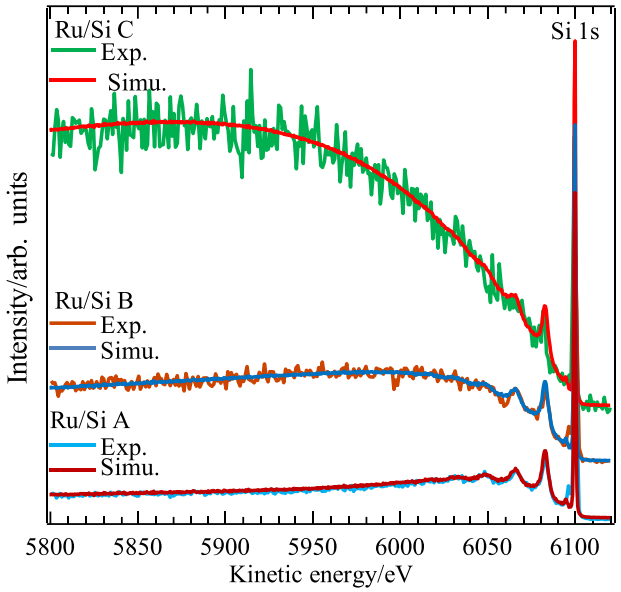

FIG. 9. The fitting results with method B around the Si 1*s* peak using a model where the Si spectrum is transported through the Ru overlayer and thus using the universal cross section in Fig. 4 valid for Ru, and IMFP = 5.68 nm (around Si 1*s*, for Ru).

well as by XPS with the peak-intensity method as described in the Appendix and elsewhere.[21] The XRR results are presented in Fig. 10. The sample thicknesses evaluated from the Ru and Si XPS peak intensities as well as the Ru/Si XPS peak-intensity ratios (calculated with the peak-area ratio of the Ru 3*d* and Si 2*p* core-level peaks) are described in the Appendix. The thicknesses from these methods are listed in Table II. Among the methods, XRR allows us to study a wide range of thicknesses due to the use of hard X-rays. The advantage of determining the thickness by XPS is that it can be applied "*in situ*" for the samples, which means that the thickness is for the same sample and exactly the same position on the sample as that used for determining electronic or chemical information from XPS. We also note that XRR can only give a large-area average thickness. From Table II, it is clear that for samples Ru/Si B and C, the thicknesses determined by the different methods are in good agreement with those obtained by the XPS-peak shape analysis (the deviations are 5%–10% for both XRR and XPS-peak intensity methods). This is because these samples are fully or nearly fully covered by the Ru film as shown by the XPS-peak shape analysis and SEM results. For sample Ru/Si A, the results from the XRR and XPS-peak intensity methods deviate more from the XPS-peak shape analysis ones. This is as expected because as the XPS peak-shape analysis shows (see Table I), the Ru film only covers 64% of the Si surface. This surface topography effect is not included in the other methods, which explains the large differences in these methods for sample Ru/Si A.

Even though the background fits and the conventional peak-ratio method (except for sample Ru/Si A) give nearly the same thickness values, the background-fitting method shows several advantages.

First, the measurement is very easy, since we do not need a special measurement setup for the reference samples and the full analysis is done with low-energy-resolution survey spectra because the energy-loss features are broad. In contrast, the reference samples needed in the peak-ratio method are affected by sample size and shape, beam size, beam intensity, and so on. It is rather difficult to do this kind of calibration for reference samples in a synchrotron-based XPS system. Furthermore, the peak-ratio method is only valid when the film covers the full substrate and gives the wrong thickness for the Ru/Si A sample.

Second, the accuracy of the background fitting is very good if the energy-loss cross section and IMFP are well known since the fits can be judged by comparing the simulated and experimental spectra. Figure 11(a) shows fits for various simulated thicknesses with a fixed IMFP of 5.68 nm ($E_k = 6050$ eV around Si 1*s*, for Ru), which illustrates that the uncertainty in the determined Ru thickness for the Ru/Si C sample is smaller than 0.2 nm even in the energy region close (energy loss <50 eV) to the photoelectron peak position. Thus, clear spectral differences from the best fit can be distinguished in Fig. 11(a) with a 0.2 nm thickness change.

Third, the IMFP can be calculated, if the film thickness is known. Figure 11(b) shows the fitted results with different IMFP values for an assumed 17.5 nm Ru thickness. The best fit is obtained with an IMFP of 5.68 nm and clearly worse fits are obtained when the IMFP is varied by only 0.1 nm from this value. Thus, the IMFP can be determined with an uncertainty of 0.1 nm. Similar analysis was done assuming that the film thicknesses are the values determined by XRR in Table II, i.e., 10.3 nm for Ru/Si B and 16.4 nm for

TABLE II. The fitting results of Ru thicknesses by Si 1*s* core-level peaks with Methods A and B, peak-intensity ratio, and XRR. The IMFPs used for the fits were 4.77 nm ($E_k = 4900$ eV around Ru $2p_{3/2}$, for Ru), 5.68 nm ($E_k = 6050$ eV around Si 1*s*, for Ru), 6.93 nm ($E_k = 7670$ eV around Ru $3d_{5/2}$, for Ru), and 7.06 nm ($E_k = 7840$ eV around Si 2*p*, for Ru), respectively.

Technique	Method	Peaks	Ru/Si A (nm)	Ru/Si B (nm)	Ru/Si C (nm)	Ru/Si D (nm)	Ru/Si E (nm)	Limit
XPS	Peak intensity	Ru 2*p*	6.5	12	17.0	>30	>30	~5 λ
		Si 1*s*	6.0	12.5	17.2	…	…	…
		by Ru/Si ratio[a]	3.4	10.3	18.2	…	…	…
	Method A	Ru 2*p*	4.2	11.7	17.0	>100	>100	~20 λ
		Si 1*s*	4.9	11.7	17.2	…	…	…
	Method B	Si 1*s*	4.7	10.6	17.5	…	…	…
XRR			3.5	10.3	16.4	113	156	…
Target thickness			3	9	15	100	150	…

[a]Calculated with peak area ratio of Ru 3*d* and Si 2*p* core-level peaks.

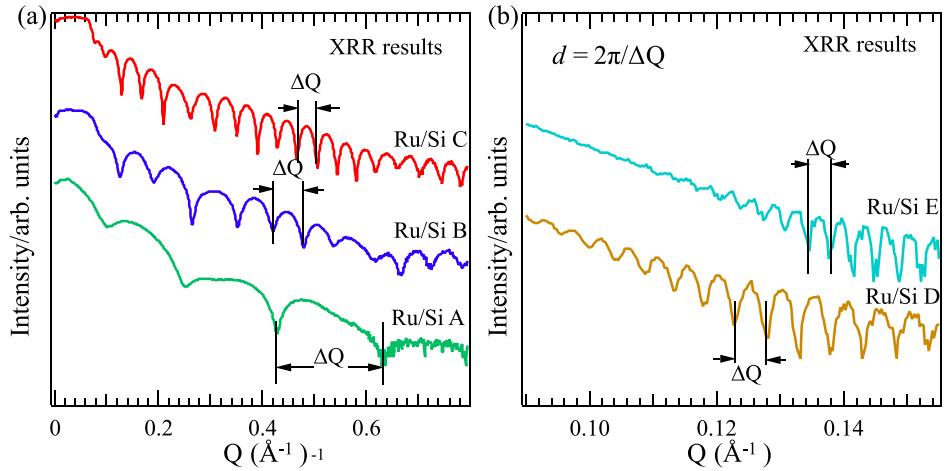

FIG. 10. The XRR results for the Ru/Si samples. (a) With synchrotron, X-ray energies of 10 keV and 12.4 keV. (b) With Cu $K\alpha$ X-rays.

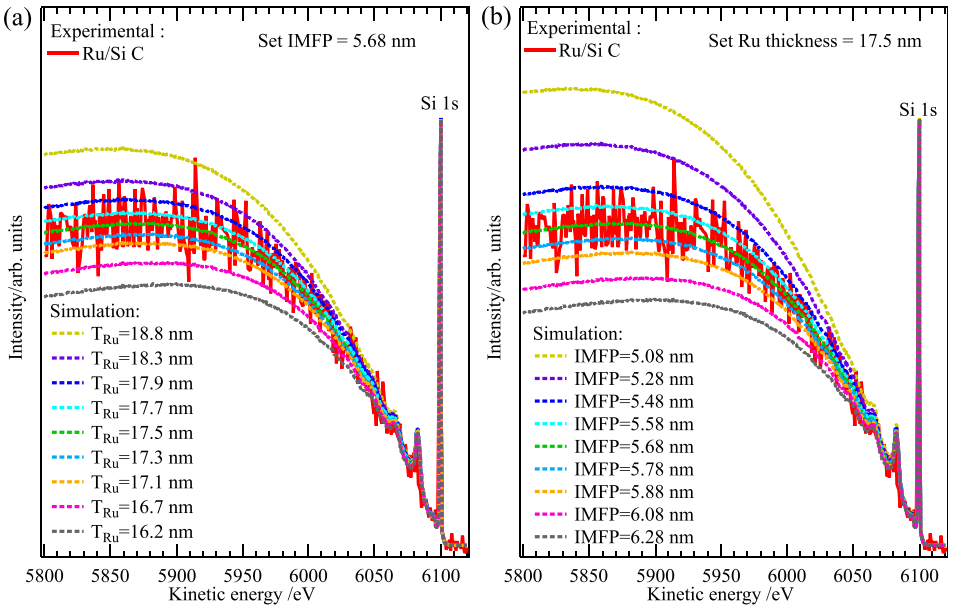

FIG. 11. Simulated results for Ru/Si C with method B. (a) The spectrum shape changes against thickness around 17.5 nm with a fixed IMFP of 5.68 nm. (b) The spectra shape changes against IMFP around 5.68 nm with a fixed Ru thickness of 17.5 nm.

Ru/Si C. The XRR value (3.5 nm) for the Ru/Si A sample was corrected to account for the fact that the Ru film forms islands with a coverage of 64% on the surface from previous analysis. The fitted IMFP values by both methods A and B are shown in Table III together with the determined IMFP values from Ref. 12 for 4900 eV and 6050 eV photo-excited electrons in Ru corresponding to the kinetic energy of the Ru 2*p* and Si 1*s*, respectively. As can be seen, the IMFP values from Ref. 12 are close to the values determined here, with deviations between 2% and 12% and a mean deviation of 7%.

One thing should be noted that for X-ray photoelectron spectroscopy with hard X-rays, the IMFP is not sensitive to kinetic energy even within several hundred eV because the very high kinetic energies of the probed photoelectrons. As for spectra around Si 1*s*, the IMFP is 5.68 nm (for the kinetic energy of 6050 eV), and even with the kinetic energy reduction of 300 eV to 5750 eV, the IMFP is still 5.45 nm, with an averaged IMFP of 5.56 nm at a centroid kinetic energy of 5900 eV. The same for the spectra around Ru 2*p*: the IMFP is around 4.77 nm at the kinetic energy of 4900 eV, and with a kinetic energy reduction of 400 eV to 4500 eV, the IMFP is changed to 4.44 nm, with an averaged IMFP of 4.65 nm at a centroid kinetic energy value of 4700 eV. The above averaged IMFP values are in the evaluated error bar regions of thicknesses or the IMFP as described in Figs. 11(a) and 11(b), respectively. Therefore, this justifies why we can use fixed IMFP values in the fits of this work.

TABLE III. Inelastic mean free paths for 4900 eV and 6050 eV electrons in Ru determined by the present methods assuming that the film thicknesses are equal to those determined by XRR (in Table II). Also shown are IMFP values from Ref. 12.

		IMFP for Ru		
Method	Sample	This work	From Ref. 12	Deviation (%)
Method A around Ru 2*p*	Ru/Si A	4.2 nm	4.77 nm	12
$E_k = 4900$ eV	Ru/Si B	4.2 nm		12
	Ru/Si C	4.4 nm		8
Method A around Si 1*s*	Ru/Si A	6.0 nm	5.68 nm	6
$E_k = 6050$ eV	Ru/Si B	5.1 nm		10
	Ru/Si C	5.4 nm		5
Method B around Si 1*s*	Ru/Si A	5.8 nm	5.68 nm	2
$E_k = 6050$ eV	Ru/Si B	5.5 nm		3
	Ru/Si C	5.3 nm		7

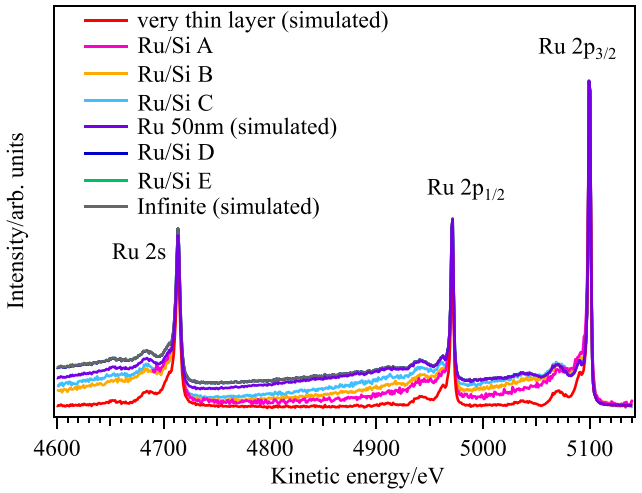

FIG. 12. The experimental and simulated backgrounds for different Ru thicknesses around the Ru 2*s*, 2*p* core-level peaks.

Fourth, background fits can give larger probing depths. Since the XPS peak intensity from the substrate decreases exponentially with depth d

$$I = I_0 \exp\left(-\frac{d}{\lambda \cos\theta}\right), \tag{5}$$

the probing depth is definitely smaller than 5 λ (>99% theoretical value) and in practice not much larger than 3 λ (>95% theoretical value). But for background fits, due to the electron energy loss, the background tail also changes for depths larger than 10 λ in the energy region far from the peak, as seen in Figs. 12 and 13. Even with a Ru thickness of more than 100 nm (>20 λ) spectral differences are seen in the energy region far below the peak energies (see Figs. 12 and 13). This situation cannot be analyzed with the peak-ratio method, since no Si 1*s* intensity can be detected as shown in Fig. 13. The demonstrated sensitivity up to ~20 λ is larger than the ~10 λ which was previously reported[2,3] for XPS with conventional Al or Mg X-ray sources. The reason is that here the peak shape can be followed over a larger energy range without disturbances of photoelectron peaks from atoms in different layers.

As mentioned above, for the background fits in this work, the IMFPs and the energy-loss cross section are the only input parameters. The IMFPs can be taken from the calculations by TPP-2M[12–14] or from tables.[12,19,22] Also, if some standard spectra with known thicknesses are measured, the IMFPs can be determined by the methods mentioned in this work. The cross section $K(T)$ is available from the universal cross sections determined for several classes of material[20] or can be determined experimentally from analysis of an electron energy-loss spectrum (EELS) using the method of Tougaard and Chorkendorff[23] as implemented in the QUASES-XS-REELS software.[19]

Besides the many advantages compared to the conventional peak-intensity ratio method, the inelastic background from photoelectron peaks can also be used as an "*in situ*" detection tool for materials investigations since the relationship of background to peak intensity is strongly correlated with the sample structure. Some possible applications are as follows:

1. Analysis of the vertical and lateral distributions of an element in sandwich structures such as electrodes or devices,[15,24] due to the large probing depth of hard X-ray photoelectron spectroscopy.
2. Evaluation of the IMFPs.
3. Evaluation of the thickness and correction for the effect of the cell membrane in ambient pressure XPS.[25]
4. Analysis of the coating features of nanomaterials, such as particle coatings, electrolyte coated samples in fuel cells or Li/Na ion batteries.
5. Measurement of X-ray absorption spectroscopy (XAS) with photoelectron or Auger electron background.[26,27]

CONCLUSION

The background from photoelectrons due to energy losses during transit from where they are excited to the sample surface is investigated by hard X-ray photoemission spectroscopy. We apply the QUASES-Tougaard software package to determine the thickness and morphology of Ru films deposited on a Si (100) substrate. Film thicknesses up to 150 nm were studied and it was demonstrated that the

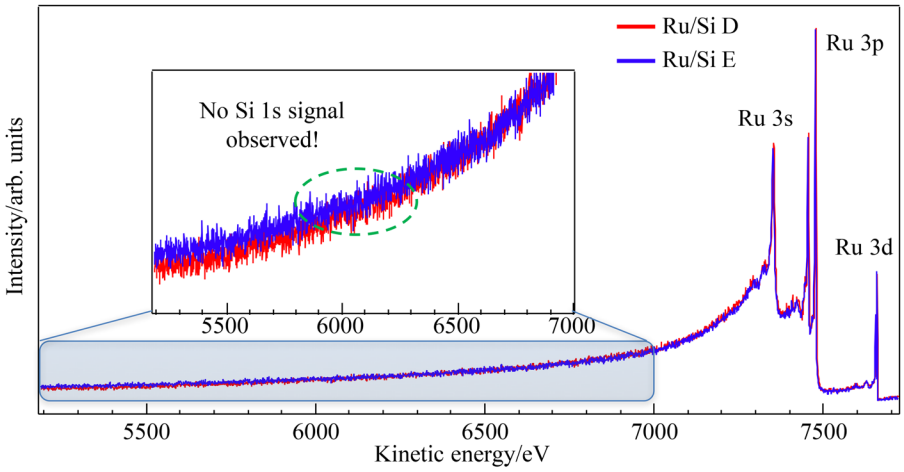

FIG. 13. The backgrounds over a wide energy region for samples Ru/Si D and Ru/Si E. The inset shows a close view around the Si 1*s* core-level peak in blue frame. No Si 1*s* was observed in the green dashed oval, but the background shows a difference even with the Ru thickness >100 nm (>20 λ). The two spectra were normalized to the same Ru 3*d* core-level peak area.

peak shape is sensitive for a thickness which corresponds to ~20 times IMFP. This is larger than the ~10 times the IMFP which has previously been reported for XPS with conventional X-ray sources and the reason is that with HAXPES, the spectrum can often be followed over a larger range of energy loss. It is found that Ru forms islands on the surface for thinner films and that it covers the complete surface for larger thicknesses. We found consistent results from analysis of the Si 1*s* peaks and the Ru 2*s*, 2*p* peaks. From the analysis of the Si 1*s* peak, we showed that because the IMFP and the inelastic cross section for Si and Ru are very different, it is more accurate to simply use the QUASES-Generate software to model the effect on the spectrum from the pure Si substrate when it is transported through the Ru overlayer. In this way, the effect of the overlayer can be calculated independent of the IMFP and cross section of the Si substrate. Good agreement in thin film thicknesses was found for the Ru film thicknesses (with deviations of 5%–12%) larger than 12 nm because the surface is completely covered while the deviation is considerable larger for smaller Ru thickness, which is expected since the surface topography by the background-analysis method revealed the formation of islands. The formation of islands was confirmed by scanning electron microscopy (SEM). It was demonstrated that the method can be used to determine the IMFP if the film thickness is known by another technique and it was applied to determine the IMFP for Ru at 4900 eV (4.3 nm) and 6050 eV (5.3 nm). Besides, some possible applications such as analysis of thin-film structure, coating features of nanomaterials, and correction for the effect of the membrane in ambient-pressure XPS are expected.

ACKNOWLEDGMENTS

We would like to thank Dr. T. Watanabe, Dr. T. Koganezawa, Dr. M. Sato of the Japan Synchrotron Radiation Institute (JASRI), Dr. Y. Katsuya of the National Institute for Materials Science (NIMS) for their kind help with XRR measurements and data analysis, and Dr. K. Funakoshi and Dr. Y. Higo of JASRI for their kind support with SEM measurements. One of the authors (Y.-T. Cui) would like to give special thanks to Professor K. Kobayashi of Japan Atomic Energy Agency (JAEA) for his warm encouragement with this work. We would like to thank the anonymous reviewers for careful review and fruitful suggestions to improve the work in clarity and style. The synchrotron-radiation experiments (for both HAXPES and XRR) were performed at beamline BL46XU of SPring-8 with the approval of the Japan Synchrotron Radiation Research Institute (JASRI) (Proposal Nos. 2011B2085, 2012A1358, 2012A1749, 2012B1244, 2013A1400, 2013B1528, 2013B1893, 2014A1774, 2014B1635, and 2014B1917).

APPENDIX: QUANTITATIVE THICKNESS ANALYSIS BY XPS PEAK INTENSITY

For a homogeneous layer of thickness d of elemental A on a substrate B, the overlayer and the substrate intensities I_A and I_B are given as follows:

$$I_A = I_{A\infty}\left[1 - \exp\left(-\frac{d}{\lambda_{A,E}\cos\theta}\right)\right], \tag{A1}$$

$$I_B = I_{B\infty}\exp\left(-\frac{d}{\lambda_{A,E}\cos\theta}\right), \tag{A2}$$

where $I_{A\infty}$ and $I_{B\infty}$ are the peak intensities from infinite thick standard samples A and B, respectively, θ is the emission angle with respect to sample normal, D is the thickness of the thin-film (A), and $\lambda_{A,E}$ is the IMFP of sample A at an electron kinetic energy E. The IMFP will vary with different kinetic energies of photoelectrons with the detection of different core-level peaks.

Therefore,

$$d = \ln\left(\frac{I_{A\infty}}{I_{A\infty} - I_A}\right)\lambda_{A,E}\cos\theta, \tag{A3}$$

$$d = \ln\left(\frac{I_{B\infty}}{I_B}\right)\lambda_{A,E}\cos\theta. \tag{A4}$$

Combining Eqs. (A3) and (A4), if the differences of IMFPs at the kinetic energy of the two measured peaks are small and can be neglected, then

$$d = \ln\left(\frac{I_A \cdot I_{B\infty}}{I_{A\infty}\cdot I_B} + 1\right)\lambda_{A,E}\cos\theta. \tag{A5}$$

Overlayer thicknesses calculated from Eqs. (A3), (A4), and (A5) are listed in Table II (marked with Peak intensity by Ru 2*p*, Si 1*s*, and Ru/Si ratio, respectively). $I_{A\infty}$ and $I_{B\infty}$ used in the calculations are from Ru films with a thickness of 155 nm and the bare Si substrate, respectively, since the thicknesses are more than 20 times the IMFP.

[1]S. Tougaard, J. Vac. Sci. Technol. A **5**, 1275 (1987).
[2]S. Tougaard, Surf. Interface Anal. **26**, 249 (1998).
[3]S. Tougaard, J. Electron Spectrosc. Relat. Phenom. **178–179**, 128 (2010).
[4]H. Kitamura, Rev. Sci. Instrum. **66**, 2007 (1995).
[5]H. Kitamura, J. Synchrotron Radiat. **7**, 121 (2000).
[6]K. Kobayashi, M. Yabashi, Y. Takata, T. Tokushima, S. Shin, K. Tamasaku, D. Miwa, T. Ishikawa, H. Nohira, T. Hattori, Y. Sugita, O. Nakatsuka, A. Sakai, and S. Zaima, Appl. Phys. Lett. **83**, 1005 (2003).
[7]Y. Takata, M. Yabashi, K. Tamasaku, Y. Nishino, D. Miwa, T. Ishikawa, E. Ikenaga, K. Horiba, S. Shin, M. Arita, K. Shimada, H. Namatame, M. Taniguchi, H. Nohira, T. Hattori, S. Södergren, B. Wannberg, and K. Kobayashi, Nucl. Instrum. Methods Phys. Res., Sect. A **547**, 50 (2005).
[8]K. Kobayashi, Nucl. Instrum. Methods Phys. Res., Sect. A **547**, 98 (2005).
[9]J. C. Woicik, *Hard X-Ray Photoelectron Spectroscopy (HAXPES)* (Springer International Publishing, Cham, 2016).
[10]K. Kobayashi, Nucl. Instrum. Methods Phys. Res., Sect. A **601**, 32 (2009).
[11]M. P. Seah and S. J. Spencer, J. Vac. Sci. Technol. A **21**, 345 (2003).
[12]S. Tanuma, C. J. Powell, and D. R. Penn, Surf. Interface Anal. **43**, 689 (2011).
[13]S. Tanuma, S. Ichimura, K. Goto, and T. Kimura, J. Surf. Anal. **9**, 285 (2002).
[14]S. Tanuma, H. Yoshikawa, H. Shinotsuka, and R. Ueda, J. Electron Spectrosc. Relat. Phenom. **190**, 127 (2013).
[15]O. Renault, C. Zborowski, P. Risterucci, C. Wiemann, G. Grenet, C. M. Schneider, and S. Tougaard, Appl. Phys. Lett. **109**, 011602 (2016).
[16]Y.-T. Cui, G. Li, H. Oji, and J. Son, J. Phys.: Conf. Ser. **502**, 012007 (2014).
[17]H. Oji, T. Matsumoto, Y.-T. Cui, and J.-Y. Son, J. Phys.: Conf. Ser. **502**, 012005 (2014).
[18]S. Goto, private communication (2012).
[19]S. Tougaard, see www.quases.com for QUASES-Tougaard: Software Packages to Characterize Surface nano-Structures by Analysis of Electron Spectra, version 6.02 (2016).

[20]S. Tougaard, Surf. Interface Anal. **25**, 137 (1997).
[21]D. Briggs and M. P. Seah, *Practical Surface Analysis* (Wiley, 1990).
[22]See https://www.nist.gov/srd/nist-Standard-Reference-Database-71 for NIST Electron Inelastic-Mean-Free-Path Database.
[23]S. Tougaard and I. Chorkendorff, Phys. Rev. B **35**, 6570 (1987).
[24]P. Risterucci, O. Renault, E. Martinez, B. Detlefs, V. Delaye, J. Zegenhagen, C. Gaumer, G. Grenet, and S. Tougaard, Appl. Phys. Lett. **104**, 051608 (2014).
[25]Y.-T. Cui, S. Tougaard, E. Ikenaga, H. Oji, J. Son, Y. Harada, and M. Oshima, "Novel XPS background analysis method developed for ambient pressure photoelectron spectroscopy" (unpublished).
[26]N. Isomura, N. Soejima, S. Iwasaki, T. Nomoto, T. Murai, and Y. Kimoto, Appl. Surf. Sci. **355**, 268 (2015).
[27]N. Isomura, Y.-T. Cui, T. Murai, H. Oji, and Y. Kimoto, "X-ray absorption spectroscopy to determine originating depth of electrons that form an inelastic background of Auger electron spectrum" (submitted).